PUBLICATION 7

Dual-band platform tolerant antennas for radio-frequency identification

In: IEEE Transactions on Antennas and Propagation 2006.
Vol. 54, No. 9, pp. 2632–2637.

Dual-Band Platform Tolerant Antennas for Radio-Frequency Identification

Mervi Hirvonen, Kaarle Jaakkola, Pekka Pursula, and Jussi Säily

***Abstract*—A technique for tuning a single-element planar inverted F-antenna (PIFA) to provide a dual-band operation is introduced. The tuning is possible due to the particular impedance level typical to radio-frequency identification microchips. As the desired impedance level resides near the outer rim of the Smith chart, a single impedance locus may be arranged to pass the input impedance twice resulting in dual-band operation. The tuning of the impedance locus is based on the feed inductance and capacitive coupling at the open end of the patch. In this paper, also a discussion about the principles of platform tolerance of small antennas is provided. A design, circuit model, simulations, and measurement results of dual-band platform tolerant PIFAs are reported and discussed.**

***Index Terms*—Dual-band, energy scavenging, planar inverted F-antenna (PIFA), platform tolerance, radio-frequency identification (RFID).**

I. Introduction

RADIO-frequency identification (RFID) has gained much interest in several service industries recently. However, for RFID tag antennas, many challenging features are required. For example, small size, low profile, direct impedance matching to the microchip, and suitability to low-cost mass production are crucial issues. Also, platform tolerance of the antenna is necessary in order to gain usability in different environments and applications. In addition, currently different frequencies are allocated for RFID use in Europe (867 MHz), North America (915 MHz), and Japan (953 MHz). Also, in RFID sensor applications, it would be beneficial to scavenge energy from radio networks in order to sustain constant sensor activity in passive systems or charge the battery in active systems. Suitable energy scavenging bands would be, for instance, the transmit frequencies allocated to GSM base stations. Thus, a multiband operation of the RFID tag antennas is preferred.

Multiband operation is traditionally achieved in antennas by using several resonant elements or exploiting the harmonics [1]. Placing several resonant elements for example in PIFA structures leads to large size. Also, coupling between the elements may degrade the performance of the antenna severely. On the other hand, by exploiting the harmonic frequencies, only multiples of the base frequency may be generated. In most cases, also different platforms tend to affect the characteristics of the antenna [2]–[6]. In this paper, the technique for tuning a single-element platform-tolerant PIFA for dual-band operation at arbitrary frequency bands is introduced.

Manuscript received September 8, 2005; revised April 5, 2006. This work was supported by Tekes (The National Technology Agency of Finland) and UPM Rafsec.

The authors are with the VTT Technical Research Centre of Finland, FI-02044 VTT, Finland (e-mail: Mervi.Hirvonen@vtt.fi).

Digital Object Identifier 10.1109/TAP.2006.880726

II. Platform Tolerance

For many antennas, the radiation pattern, bandwidth, and input impedance are typically highly platform dependent. However, in RFID applications the same antenna type may be attached directly on top of different kinds of objects. Especially stable impedance behavior is essential, since the power supply of the RFID microchip depends greatly on matching. Traditionally, the effects of the platform to antenna impedance are decreased by using large ground planes in the antenna structure. For example, according to [2]–[4], a ground plane of wavelengths in size is needed to stabilize the input impedance of a vertical monopole. Also, results concerning circular microstrip antennas have been reported in [5]. The study shows that a ground plane radius beyond 1.3 times the patch radius is enough to stabilize the input impedance. A similar study concerning a PIFA structure has been reported in [6], where the ground plane of only less than 0.2λ in size had an impact on the input impedance. Still, the exact size of the ground plane needed to stabilize the input impedance of the antenna depends also on the impedance bandwidth. Broad bandwidth is thus another technique to minimize the platform effects. However, in small antenna structures like PIFAs, broad bandwidth usually means large size and more importantly, high profile. For example, the PIFA introduced in [6] is 0.065λ high, which is unacceptable in RFID applications.

Regardless of the antenna bandwidth, platform-tolerant impedance behavior may also be achieved with a certain current distribution. It has been presented that surface currents induced by horizontal point sources above the ground plane decay more rapidly than those induced by vertical sources [7]. In other words, e.g., PIFA structures with dominating horizontal current distribution tend to be more platform tolerant than those with dominating vertical sources. Of course, the proximity of the ground plane for dominating horizontal current leads to very narrow bandwidth behavior, but in RFID applications only a narrow operation band is required. Dominating vertical current distribution is typical to many PIFA structures, since a vertical short tends to attract the current. However, by widening the short, i.e., reducing the inductance of the vertical part and lowering the height of the antenna, a dominating horizontal current distribution is achievable [8].

III. Dual-Band Operation

In RFID applications, the antenna is connected to a microchip. In order to maximize the power supply of the chip,

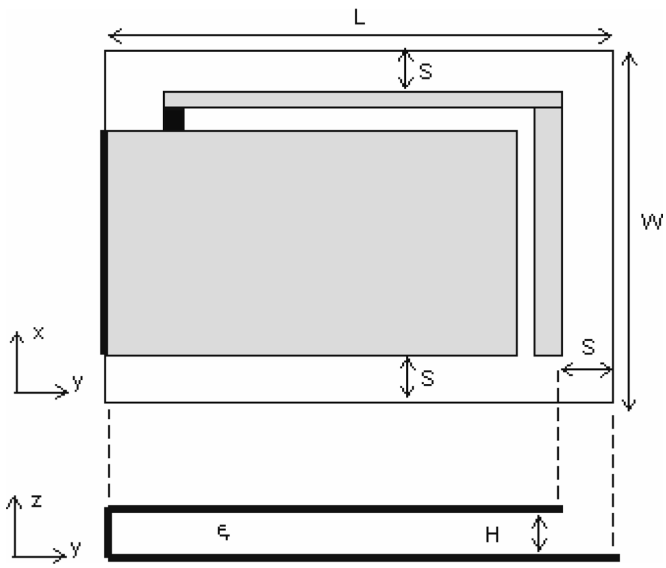

Fig. 1. Dual-band PIFA design.

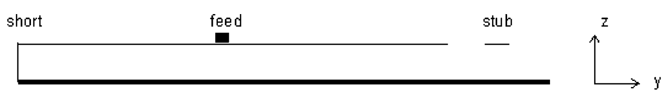

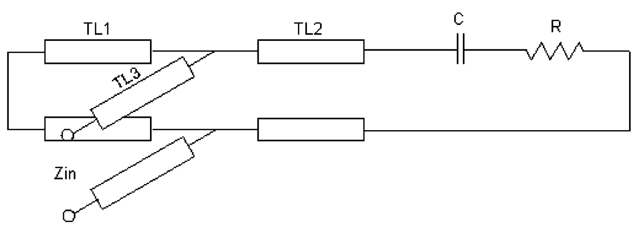

Fig. 2. Equivalent circuit of the proposed PIFA structure.

the RFID antennas are directly conjugately matched to the microchip terminal impedance. The impedance of the RFID microchips usually behaves as a series RC-circuit. In practice, this means a large reactive part of the impedance [9]. On the other hand, the real part of the impedance is quite low. The required input impedance of the RFID antenna is thus typically between (5-30)+j(130-250) Ω.

Like microstrip antennas, PIFA structures are typically modeled as parallel resonant circuits [10], [11]. However, in these cases, the PIFA structures are fed by 50 Ω coaxial probes. In RFID applications, the feed of the antenna is a microchip. The ground of the microchip may be arranged by via or, more importantly, by an open-ended stub as presented in Fig. 1. The use of an open-ended stub instead of a ground via is often preferred in RFID PIFA structures because of the manufacturing issues.

As the open-ended stub may be bent near the radiating edge of the patch, a series capacitance is formed instead of a parallel one. The equivalent circuit for this kind of PIFA structure is presented in Fig. 2. Transmission line 1 (TL1) defines the distance from the feed point to the short and transmission line 2 (TL2) the distance from the feed point to the open end of the patch. Transmission line 3 (TL3) represents the feed inductance relating to the length and width of the open-ended stub.

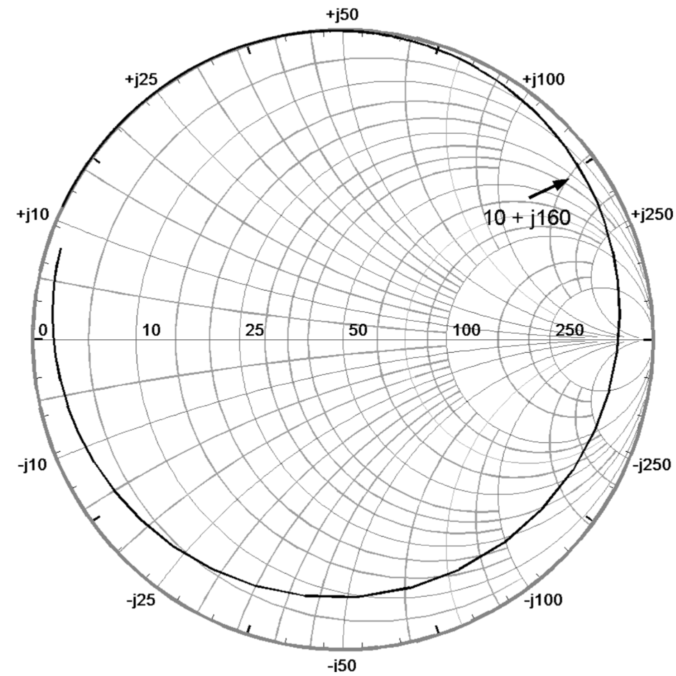

Fig. 3. Typical impedance behavior in the probe or microchip with a via fed PIFA.

In the typical case, where the antenna is fed by a probe or the ground of the microchip is arranged with a via, the feed inductance caused by TL3 is not easily tuned. In other words, the location of the impedance locus on the Smith chart is somewhat fixed. Hence, the desired input impedance may be achieved only by tuning the location of the feed (TL1 and TL2). In practice, reaching the low real impedance and highly inductive reactance usually means rather large locus, and the feed of the antenna has to be far away from the short and near the open end of the patch $(\mathrm{TL1} \gg \mathrm{TL2})$. The typical matching case is illustrated in Fig. 3. The frequency range is from 500 to 1500 MHz. As can be seen from Fig. 3, the locus passes the example input impedance 10+j160 typical to RFID only once, indicating single-band operation.

On the other hand, in the case of an open-ended stub, the length and width of the stub relate to the feed inductance TL3 and move the locus towards the load as presented in Fig. 4. In this case, the desired input impedance may be achieved with an arbitrary size impedance locus, which is moved suitably towards the load. As in RFID, the desired input impedance resides near the outer rim of the Smith chart, the impedance locus may be placed such that it passes near the desired impedance point twice, as illustrated in Fig. 4 case 3TL3. Thus, a dual-band operation may be achieved with only one resonant element. Series capacitance relates to the size of the locus as presented in Fig. 5. As the capacitance increases, a narrower frequency range forms the locus. In other words, the vicinity of the two frequency bands may be tuned by altering the coupling between the open-ended stub and the radiating edge of the patch. In practice, tuning the parameters affects the overall current distribution of the antenna. Thus, the circuit model only gives reasoning behind the dual-band tuning technique but is not suited for exact calculation.

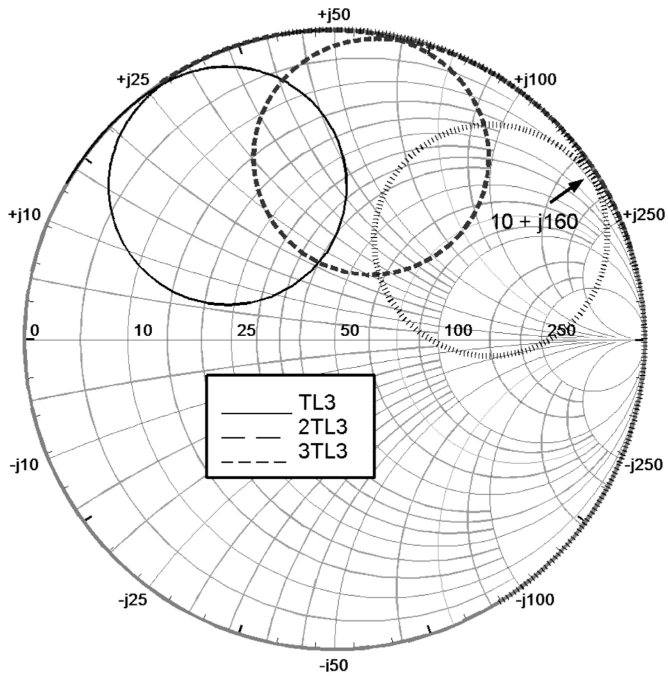

Fig. 4. Impedance behavior as a function of the length of the open-ended stub.

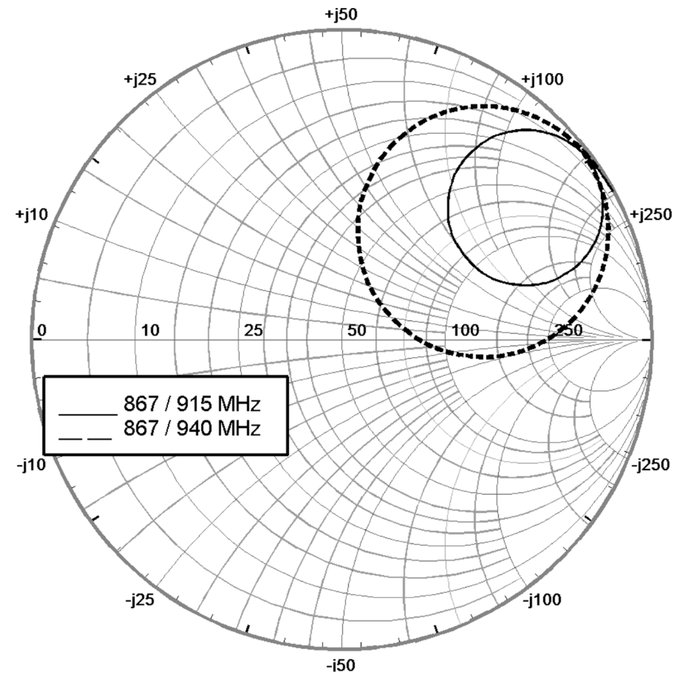

Fig. 6. Simulated input impedance.

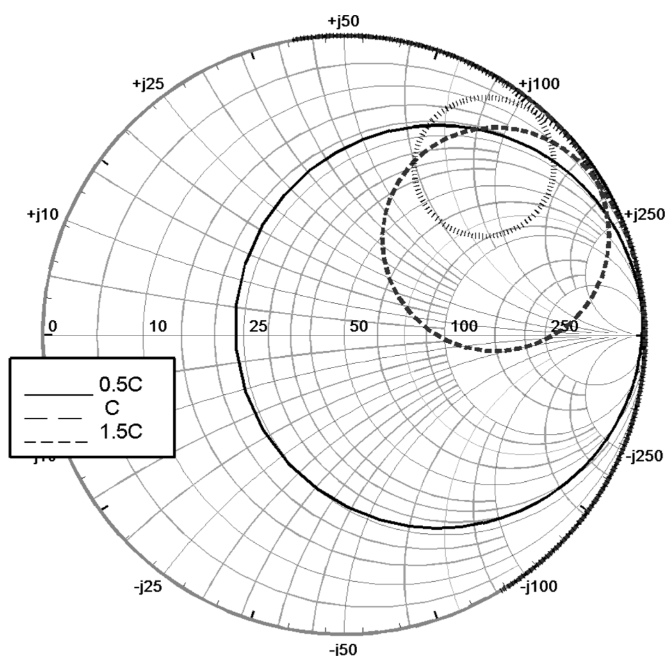

Fig. 5. Impedance behavior as a function of the series capacitance.

IV. Simulations and Measurements

The geometry of a dual-band platform-tolerant planar inverted F-antenna is presented in Fig. 1. As discussed in Section II, for achieving platform tolerance, the short is as wide as the patch edge and the antenna is really low in profile. More importantly, no ground plane is needed behind the short in order to achieve platform tolerance, which is a great asset in manufacturing. The ground of the microchip is arranged with an open ended stub in order to achieve dual-band operation as discussed in Section III.

The proposed antenna may be tuned to provide a dual-band operation for any frequency combination related to RFID. In this paper, two example cases are introduced: RFID use in Europe and in North America (867/915 MHz) and RFID use and energy scavenging in Europe (867/940 MHz). With a polyethylene substrate, $\varepsilon_{\rm r} = 2.35$, $\tan\delta = 0.002$, the length L of the antenna is 62.0 mm and width W is 51.3 mm including the ground plane. The metallization is 18-μm-thick copper. The height H of the antenna is only 3.0 mm, and 5.0 mm of ground plane frame S is needed to achieve the platform tolerance. The dimensions of the upper patch are 53.0×38.5 mm^2. In the case of a 867/915 MHz antenna, the gap between the stub and the edge of the patch is 1.0 mm, which is 0.9 mm narrower compared to the 867/940 MHz antenna, providing larger capacitance and thus more adjacent operating bands.

The simulated impedance behaviors between 850–955 MHz of the antennas are presented in Figs. 6 and 7. The simulations were conducted with Zeland IE3D software based on method of moments (MoM). The impedance of the RFID microchip in question behaves as a series RC-circuit with input impedances of (10−j160) Ω at 867 MHz, (10−j150) at 915 MHz and (10−j145) at 940 MHz. As can be seen from Fig. 6, the impedance loci pass near the desired impedance level twice providing dual-band operation. The impedance mismatch η is presented in Fig. 7.

The simulated radiation patterns are presented in Fig. 8. The patterns are the same at 867 MHz for both example antennas. As can be seen from Fig. 8, the patterns look quite similar for all the studied frequencies. The radiation is almost omnidirectional, including a strong backlobe. Also, the radiation is highly linearly polarized, resembling the radiation of a loop or magnetic dipole due to the dominating horizontal current distribution.

The impedance matchings of the antennas were verified with a scattering measurement technique [12]. A test microchip was

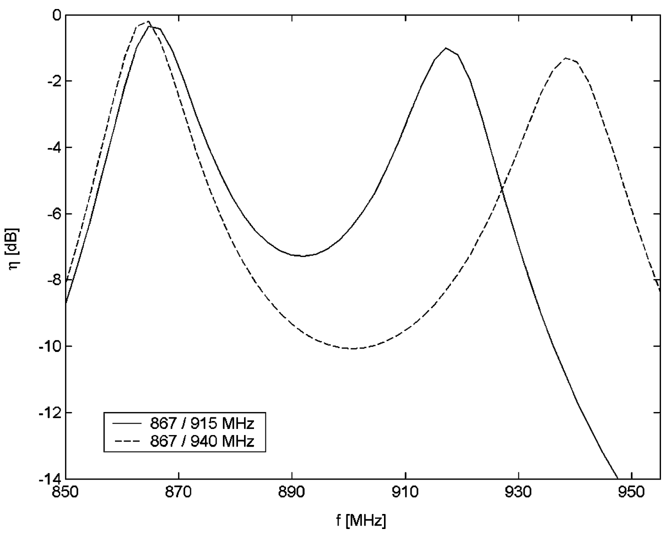

Fig. 7. Simulated impedance mismatch.

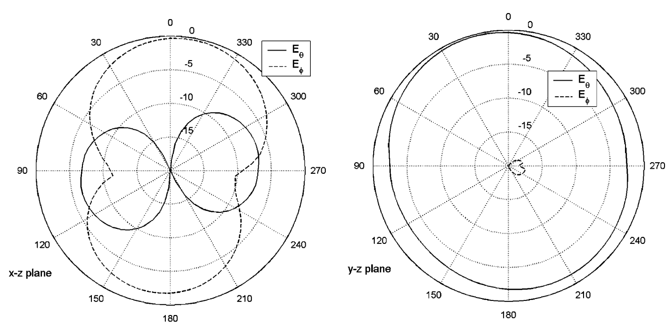

a)

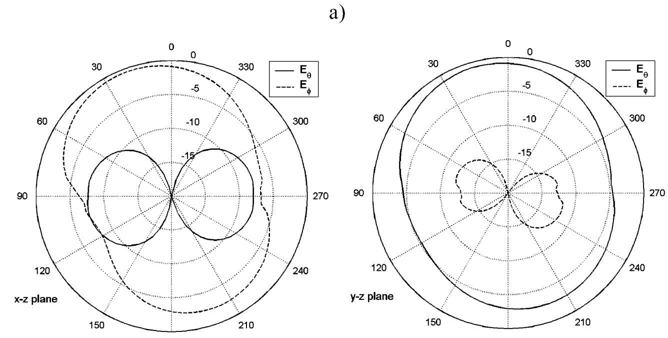

b)

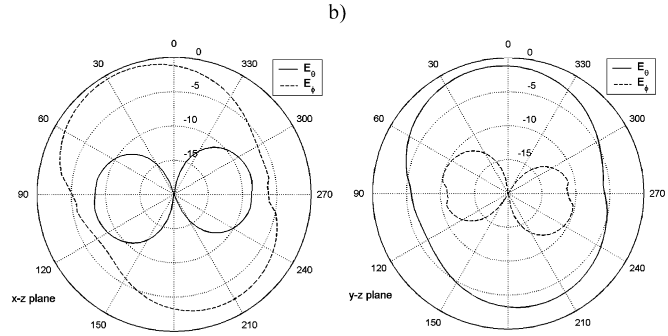

c)

Fig. 8. Simulated radiation patterns at (a) 867 MHz, (b) 915 MHz, and (c) 940 MHz.

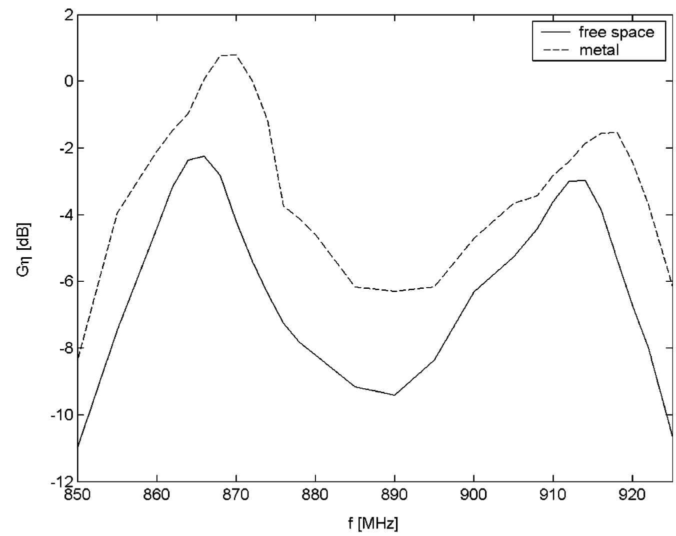

Fig. 9. Measured gain including mismatch of the 867/915 MHz antenna.

connected as a load to the antenna. The chip contains an oscillator that drives a varactor at the input of the chip, causing a phase modulation of the backscattered signal. The modulation starts if the chip is fed at least with $P_{req} = 16\ \mu$W of input RF power. Because this limiting power is constant, the transmit power P_{tx} needed to wake up the modulation describes the power transfer between the antenna and the chip. The lower the required transmit power P_{tx}, the better the matching between the antenna and the chip. In fact, the effective antenna aperture A_e including the mismatch η between the antenna and the load is inversely proportional to the required transmit power P_{tx}

$$A_e\eta = \frac{\lambda^2 G}{4\pi}\eta = \frac{P_{req}}{S} = \frac{4\pi r^2 P_{req}}{G_{tx}P_{tx}} \tag{1}$$

where S describes the power density of the transmitted field at a distance r. Measuring the required transmit power as a function of the frequency gives information of the antenna bandwidth with the microchip as its load. The oscillator chip has the same input impedance as the RFID chip, with which the antenna will be used. Thus, the measurement describes the antenna in the actual application.

The results of the scattering measurements, in other words, gain including the impedance mismatch between the antenna and the chip, are presented in Figs. 9 and 10. Polarization mismatch is neglected. As can be seen from Fig. 9, two separate bands are detected at 867 and 915 MHz, and the bandwidths are around 14 MHz. The bandwidth is defined as a half-power bandwidth of the antenna gain. The results for the 867/940 MHz antenna are quite similar. Two distinct bands are detected with bandwidths around 13 MHz. As can be seen from both cases, the center frequencies of the bands are about the same for the measurements done in free space and for the measurement, where the antennas were placed directly on top of a 46×46 cm^2 metal plate. The results indicate very good tolerance to platform. The gain levels are higher for the results on metal as expected because of the increased directivity.

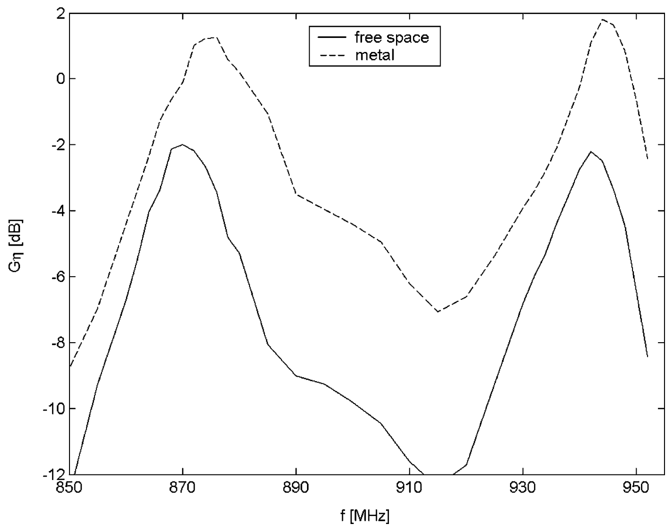

Fig. 10. Measured gain including mismatch of the 867/940 MHz antenna.

TABLE I
RADIATION CHARACTERISTICS

	867 MHz	915 MHz	940 MHz
D_{sim} [dB]	2.3	2.7	2.8
$\eta_{eff,\ sim}$	0.36	0.32	0.31
G_{sim} [dB]	-2.1	-2.2	-2.3
$G\eta_{mes}$ [dB]	-2.2	-2.9	-2.2

TABLE II
CALCULATED AND MEASURED READ-RANGES

	867 MHz	869 MHz	915 MHz
$r_{cal,\ free\ space}$ [m]	9.7	4.8	9.3
$r_{mes,\ free\ space}$ [m]	7.0	3.5	N/A
$r_{cal,\ metal}$ [m]	13.7	6.8	13.2
$r_{mes,\ metal}$ [m]	10.9	5.6	N/A

The radiation characteristics of the antennas in free space are presented in Table I. The values are about the same for both antennas at 867 MHz. According to the simulation results, the directivity and radiation efficiency are low. Simulated and measured gain values correspond well, even though these parameters are not fully comparable, since impedance mismatch is included in the measurement results.

The calculated and measured read-ranges of the developed antennas are presented in Table II. The calculated read-ranges at 867 MHz (ETSI 2 W ERP), 869 MHz (ETSI 0.5 W ERP), and 915 MHz (FCC 4 W EIRP) are based on measured gain values $G\eta$ and calculation on (1). The read-range measurements were conducted with a Deister UDL 500 reader device at the entrance hall of a block of offices. In other words, the measured values correspond to a reliable and reproducible maximum reading distance in a real application environment. The measurements were conducted only with the two European bands, since frequency allocation issues prevented the measurements in the 915 MHz band. As expected, the measured ranges are shorter than the calculated ones because of multipath propagation.

V. CONCLUSIONS

In this paper, a dual-band platform-tolerant single element PIFA structure has been introduced. Platform tolerance of the structure is achieved by utilizing dominating horizontal current distribution. The dual-band operation at frequencies related to RFID is achieved by exploiting the particular impedance level typical to RFID microchips. The tunable feed inductance and the series capacitance at the radiating edge of the patch play the key roles in the dual-band operation. Simulations and measurements are presented for two example antennas, showing good correlation. Also, the presence of metal is demonstrated not to have any significant effect on antenna matching performance. Thus, the structure is expected to be useful in many different RFID applications and on several continents.

REFERENCES

[1] K.-L. Wong, *Planar Antennas for Wireless Communications*. New York: Wiley, 2003.
[2] A. S. Meier and W. P. Summers, "Measured impedance of vertical antennas over finite ground planes," *Proc. IEEE*, vol. 37, pp. 609–616, Jun. 1949.
[3] K. H. Awadalla and T. S. M. Maclean, "Input impedance of a monopole antenna at the center of a finite ground plane," *IEEE Trans. Antennas Propag.*, vol. AP-26, pp. 244–248, Mar. 1978.
[4] J. H. Richmond, "Monopole antenna on circular disk," *IEEE Trans. Antennas Propag.*, vol. AP-32, pp. 1282–1287, Dec. 1984.
[5] K. Antoszkiewicz and L. Shafai, "Impedance characteristics of circular microstrip patches," *IEEE Trans. Antennas Propag.*, vol. AP-38, pp. 942–946, Jun. 1990.
[6] M.-C. Huynh and W. Stutzman, "Ground plane effects on planar inverted-F antenna (PIFA) performance," *Proc. Inst. Elect. Eng. Microw. Antennas Propag.*, vol. 150, no. 4, pp. 209–213, Aug. 2003.
[7] J. C.-E. Sten and M. Hirvonen, "Decay of groundplane currents of small antenna elements," *IEEE Antennas Wireless Propag. Lett.*, vol. 4, pp. 82–84, 2005.
[8] M. Hirvonen, P. Pursula, K. Jaakkola, and K. Laukkanen, "Planar inverted F-antenna for radio frequency identification," *Electron. Lett.*, vol. 40, no. 14, pp. 848–850, Jul. 2004.
[9] U. Karthaus and M. Fischer, "Fully integrated passive UHF RFID transponder IC with 16.7-μW minimum RF input power," *IEEE J. Solid-State Circuits*, vol. 38, pp. 1602–1608, Oct. 2003.
[10] K. Hirasawa and M. Haneishi, *Analysis, Design, and Measurement of Small and Low-Profile Antennas*. Norwood, MA: Artech House, 1992.
[11] J. Ollikainen, "Design and implementation techniques of wideband mobile communications antennas" Ph.D. dissertation, Helsinki Univ. of Technology, Espoo, Nov. 2004 [Online]. Available: http://www. lib. tkk.fi/Diss/2004/isbn9512273810
[12] P. Pursula, T. Varpula, K. Jaakkola, and M. Hirvonen, "Antenna radiation characterization by backscattering modulation," in *URSI/IEEE XXIX Nat. Conv. Radio Science, VTT Symp. 235*, Nov. 2004 [Online]. Available: http://www.vtt.fi/inf/pdf/symposiums/2004/S235.pdf

Mervi Hirvonen was born in Espoo, Finland, in 1980. She received the master of science (Tech.) degree in electrical engineering from Helsinki University of Technology (TKK), Espoo, Finland, in 2004.

Since 2002, she has been with the VTT Technical Research Centre of Finland, initially as a Research Trainee and, since 2004, as a Research Scientist. Her current research interests include antennas and electromagnetics related to wireless sensors, RFID systems, and mobile communications.

Kaarle Jaakkola was born in Helsinki, Finland, in 1976. He received the master of science (Tech.) degree in electrical engineering from Helsinki University of Technology (TKK), Espoo, Finland, in 2003.

Since 2000, he has been with the VTT Technical Research Centre of Finland, first as a Research Trainee and, since 2003, as a Research Scientist. In 2000–2002, he participated in the Palomar (EC IST) project developing RF parts for a new RFID system. His current research interests include RFID systems, wireless and applied sensors, antennas, electromagnetic modelling, and RF electronics.

Pekka Pursula was born in Vantaa, Finland, in 1978. He received the master of science (Tech.) degree (with distinction) in technical physics from Helsinki University of Technology (TKK), Espoo, Finland, in 2002.

In 2002, he was with Philips Medical Systems Finland developing RF systems in magnetic resonance imaging. Since 2003, he has been with the VTT Technical Research Centre of Finland. His present research interests include RFID systems and wireless sensors.

Mr. Pursula received the Young Scientist Award at the URSI/IEEE XXIX Convention on Radio Science, Espoo, Finland, in November 2004.

Jussi Säily was born in Rantsila, Finland, in 1974. He received the master of science (Tech.), licentiate of science (Tech.), and doctor of science (Tech.) degrees in electrical engineering from Helsinki University of Technology (TKK), Espoo, Finland, in 1997, 2000, and 2003, respectively.

In 1996, he was a Research Trainee with the Automation/Measurement Technology Laboratory, VTT Technical Research Centre Finland, where he studied microelectromechanical sensors. From 1997 to 2003, he was a Research Engineer with the Radio Laboratory, TKK, where he studied, e.g., phase-locked millimeter- and submillimeter-wave signal sources and receivers for antenna measurements. Since 2004, he has been with the Circuits and Antennas Knowledge Centre (formerly the Antennas and Electromagnetics Research Group), VTT, where he is currently a Senior Research Scientist. His current research interests include beam-steerable millimeter-wave antenna arrays for short-range communications, smart base-station antenna arrays for telecommunications, RFID antennas, and low-noise signal sources for instrumentation.